Pergamon

0301-9322(93)E0023-X

Int. J. Multiphase Flow Vol. 20, No. 3, pp. 515–522, 1994

0301-9322/94 $7.00 + 0.00

PRESSURE DROP AT ROD-BUNDLE SPACERS IN THE POST-CHF DISPERSED FLOW REGIME

C. UNAL,[1] O. BADR,[2] K. TUZLA,[3] J. C. CHEN[3] and S. NETI[3]

[1]Science Applications International Corporation, Los Alamos National Laboratory, Mail Stop K555, Los Alamos, NM 87545, U.S.A.

[2]UAE University, Al-Ain, P.O. Box 17555, United Arab Emirates

[3]Institute of Thermo-Fluid Engineering and Science, Lehigh University, Bethlehem, PA 18015, U.S.A.

(Received 28 December 1992; in revised form 24 November 1993)

Abstract—The axial pressure drop for two-phase post-CHF dispersed flow along a rod bundle with a straight grid spacer was investigated experimentally. Thermodynamic non-equilibrium was considered in both the measurements and data analysis. The effects of Reynolds number and actual quality on the spacer pressure drop were also investigated. Experimental data on the frictional pressure drop in the unblocked section (e.g. without spacer) compared favorably with four well-known models. On the other hand, all available models substantially underpredicted the experimental pressure drop at the grid spacer. These deviations were attributed mainly to differences in flow patterns and heating conditions (diabatic vs adiabatic). Pressure drop values which are 300% higher than those predicted by Beattie's model were suggested for post-CHF dispersed flow in straight grid spacers.

Key Words: pressure drop, grid spacer, rod bundle, dispersed flow

INTRODUCTION

The relative position of rods in rod bundles is usually maintained by spacers. In general, spacers act as flow obstructions within the bundle and cause additional pressure drop and heat transfer augmentation. The single-phase pressure drop in rod bundles with grid spacers was correlated to some flow and geometrical parameters in the form of a loss coefficient (De Stordeur 1961; Sangster 1968; Rehme 1973, 1977; Yao *et al.* 1982). Rehme (1973, 1977) correlated the spacer loss coefficient in terms of the spacer blockage ratio, ε. Yao *et al.* (1982) carefully compared their single-phase experimental data to Rehme's (1977) correlations and found that 50% higher values for the loss coefficient appeared to be more appropriate.

Unlike in single-phase flow, flow patterns and heat transfer mechanisms in the two-phase dispersed flow regime in rod bundles with grid spacers are not clearly identified and experimental data with detailed information are very limited. Beattie (1973) reported two-phase pressure drop correlations in the form of two-phase multipliers and pressure loss coefficients for different flow patterns and geometries including pipes, pipe fittings, orifices, rod spacers and expanders. However, Beattie's (1973) boundary conditons, detailed geometries and assumptions were not clearly identified.

It is important for design calculations to know good approximations for the pressure drop in the spacer before deciding on the design of the grid. For this reason and due to the lack of knowledge of the complicated mechanisms involved, the main objective of the present paper was to perform an experimental investigation of the two-phase pressure drop in rod bundles with grid spacers in the post-CHF dispersed flow regime. Heat transfer data obtained from the present experimental program has been reported elsewhere (Unal *et al.* 1988a, b, 1991a). The emphasis of the present paper is on pressure drop measurements.

EXPERIMENTAL

The test section consisted of a heated shroud containing a 3 × 3 rod bundle assembly with a mean hydraulic diameter of 11.2 mm. A schematic diagram of the test section elevation (see figure 1)

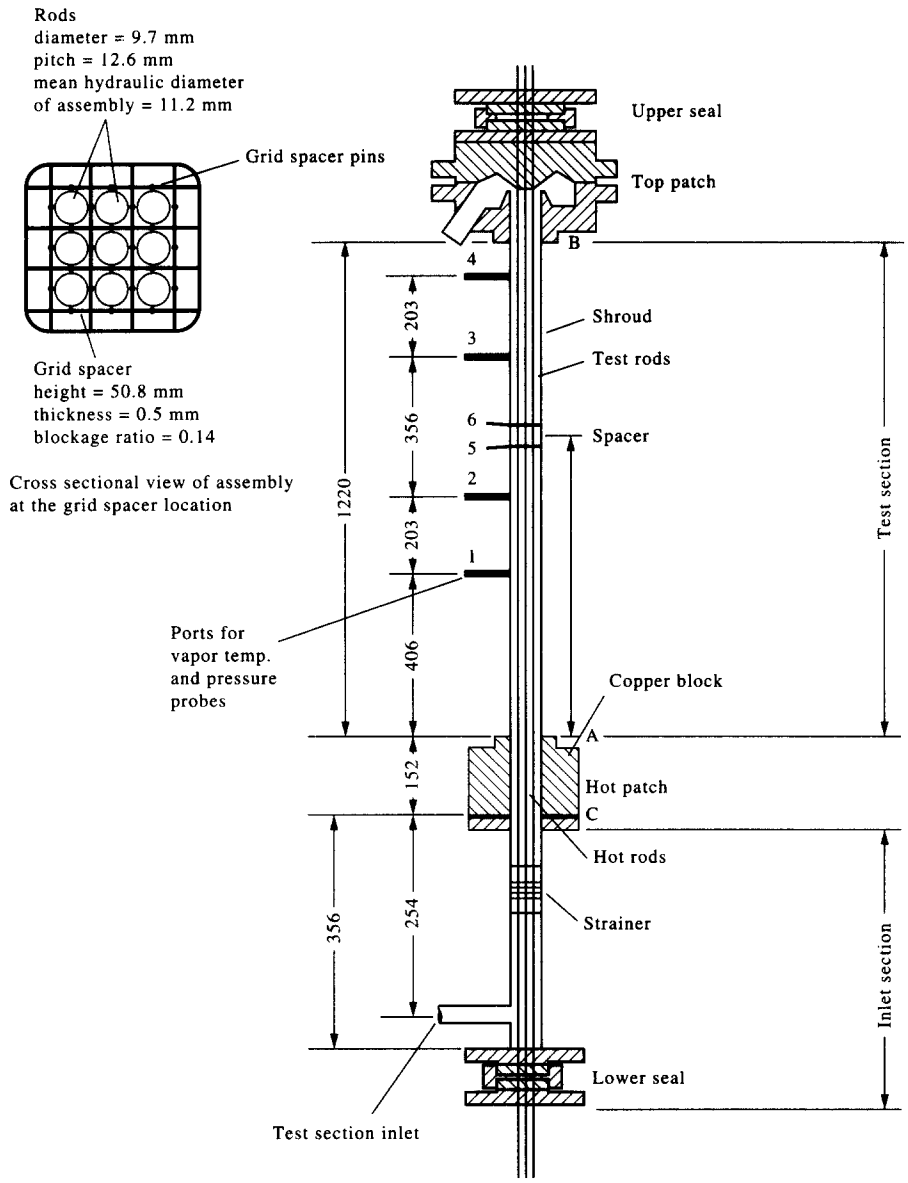

Figure 1. Schematic diagram of the test section and grid spacer.

shows an actual length (A–B) of 1.22 m with a grid spacer installed 762 mm away from the inlet point (A). The grid spacer, with a height of 50.8 mm, was made of 0.5 mm thick sheet metal which caused a blockage ratio of $\varepsilon = 0.14$, as shown in figure 1. Four ports on one side of the shroud were used for the measurements of absolute pressure, pressure differences and vapor temperatures. The shroud, made of a 2.0 mm thick sheet of Inconnel 625 alloy, was heated by a radiation furnace. The test rods were electrically heated with uniform heat flux.

Upper and lower hot patches were used to prevent quench fronts from propagating upwards and downwards along the test section, respectively. Thus, the dryout point was held at the test section inlet and stabilized post-CHF conditions within the test section were maintained. Miniature vapor probes, made of two concentric tubes with nominal diameters of 2.13 and 1.25 mm and a 0.254 mm diameter type K thermocouple placed in the center, were installed in ports 2 and 3 (see figure 1) for the measurements of non-equilibrium vapor temperatures. Moreover, the axial variation of the wall temperature was measured using 12 thermocouples on the shroud and on each of the 9 test rods.

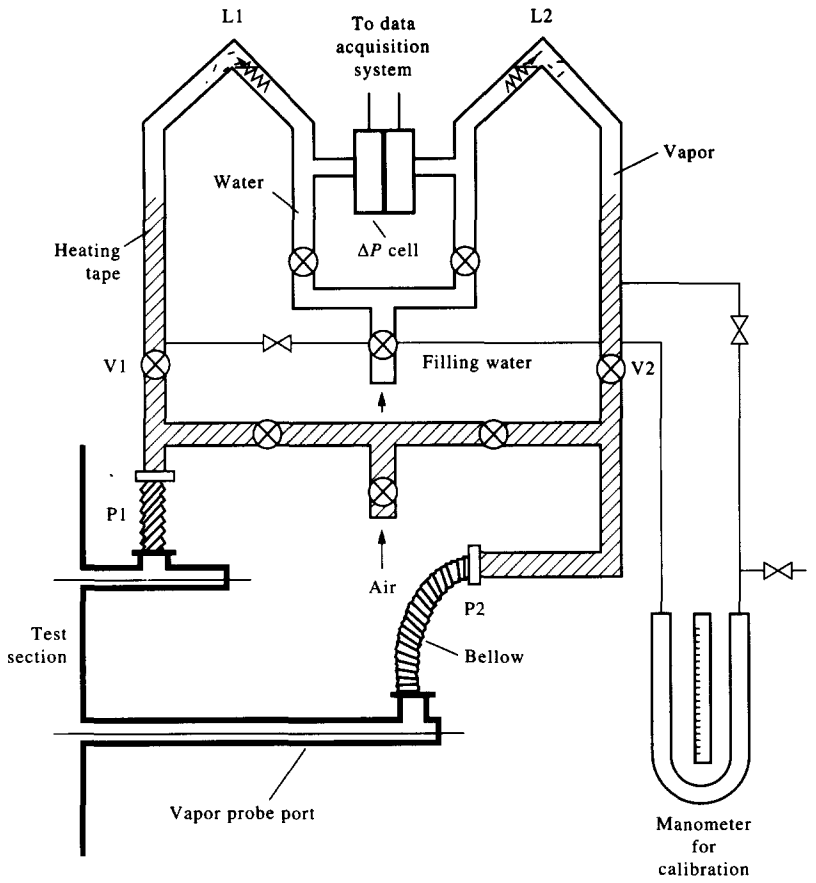

Figure 2. Schematic diagram of the pressure drop measuring system.

A schematic diagram of the pressure drop measuring system is shown in figure 2. This system is designed to eliminate the condensation of steam in the pressure transducer cell (Badr *et al.* 1993). To avoid liquid blockage, these lines were heated to temperatures high enough to vaporize any falling condensate. Compressed air was used to clean the lines between different experiments with the transducers isolated from the test section. The transducer calibration was checked periodically between experiments. The output signals of the transducers were stored on a fast data acquisition system with a rate of 100 Hz.

The uncertainty in the wall temperature measurements was $\pm 2.2°C$. The saturation temperature was measured with a $\pm 0.5°C$ uncertainty. The vapor temperature measurements included additional uncertainties, $\pm 10°C$, due to the strip chart reading and the quality of the vapor probe response. The pressure transducers had linearities of $\pm 0.5\%$ of full scale with $< 0.5\%$ zero shift for 200% overpressure. The additional uncertainty in the pressure drop measurements, due to the operation of the test setup was determined to be approximately $\pm 15\%$.

The experimental range included conditions pertinent to the reflood and quench phases of light water reactor accident analysis. The measured data are tabulated in table 1. More details pertaining to the design of the test section and the two-phase loop, instrumentation and the operating procedures are presented elsewhere (Unal *et al.* 1986, 1988a, 1991a).

RESULTS AND DISCUSSION

Our main objective is to obtain the pressure drop data across the spacer which was not directly measured. The spacer pressure drop can be obtained from the data measured between ports 2 and 3 by subtracting the gravitational, accelerational and frictional pressure drops in the unblocked parts of this rod-bundle section (the sections between points 2–5 and 6–3 in figure 1). Thus, we will first examine the pressure drop measurements obtained in the bare rod bundle (ports 1 and

Table 1. Experimental data

Test No.	G (kg/m^{2}s)	q (W/cm^2)	X_{in} or T_{in} (°C)	X_{inh}	$T_{v,1}$ (°C)	$T_{v,2}$ (°C)	ΔP_{2-3} (mmH$_2$O)	ΔP_{1-2} (mmH$_2$O)
1	15	2.6	0.22	0.45	561	366	490	—
2	15	2.6	0.22	0.46	554	361	491.6	—
3	15	2.63	0.047	0.27	689	603	319.4	—
4	15	2.63	0.047	0.27	689	588	323.5	—
5	15	2.63	0.047	0.28	713	619	323.4	—
7	19	2.63	0.18	0.41	453	246	699.6	—
8	19	3.79	0.18	0.41	568	284	625.5	—
9	19	4.44	0.18	0.41	624	279	684.8	—
10	20	3.4	0.27	0.49	453	212	684.8	—
41	12	2.01	0.21	0.38	630	555	244.7	—
42	12	2	0.21	0.47	558	512	341.6	—
44	11	2.01	0.22	0.45	623	649	342.6	—
45	11	1.93	0.22	0.46	558	507	329.4	56.0
46	11	2.05	0.22	0.45	603	565	324.3	57.6
47	12	2.46	0.012	0.24	724	657	257.1	85.3
48	12	2.16	95.5	0.22	587	616	296.0	87.8
49	12	2.21	96.5	0.28	618	613	271.2	104.7
50	12	2.21	96.5	0.28	618	594	271.2	104.7
51	17	2.79	0.33	0.53	425	459	308.1	142.5
52	17	3.82	0.4	0.62	483	516	666.8	160.2
53	12	2.55	0.2	0.47	603	691	365.5	—
54	12	2.55	0.2	0.42	603	739	341.6	—
56	12	2.27	0.2	0.47	603	520	343.9	—
57	12	2.55	0.2	0.48	631	583	329.1	46.1
58	12	2.54	0.2	0.47	631	576	369.1	36.9
59	12	2.53	0.2	0.46	619	557	341.9	34.4
60	12	2.55	0.32	0.58	588	600	392.5	35.4
61	12	2.54	0.33	0.59	579	600	403.8	35.3
62	12	2.55	0.33	0.59	579	576	421.7	33.4
63	8.8	2.12	0.2	0.48	654	734	226.2	51.4
64	8.8	2.12	0.2	0.48	664	720	226.2	51.4
66	8.8	2.11	0.09	0.4	676	754	197.8	40.0
68	8.7	1.97	0.2	0.5	640	533	262.1	33.9
69	8.5	1.96	0.22	0.52	655	681	215.2	58.4
71	8.6	2.45	0.092	0.44	686	591	239.6	52.0
72	8.6	2.07	84.4	0.38	671	686	185.5	77.6
73	8.5	2.06	84.2	0.45	647	712	201.2	82.3
74	8.5	2.07	66.9	0.36	671	750	226.3	53.0
75	8.5	2.05	66.5	0.44	617	703	190.8	63.7
76	8.5	2.05	66.6	0.34	627	725	202.7	78.6
77	8.4	2.21	50.4	0.4	644	747	203.4	69.4
78	8.5	2.2	50.1	0.41	650	747	205	63.4
79	9.0	2.21	0.36	0.63	659	585	440.8	—
86	8.7	1.64	56.4	0.33	630	724	163.4	—
87	12	2.58	0.3	0.53	604	559	367.5	—
88	9.1	1.62	0.45	0.67	529	517	287.1	—
89	12	2.37	0.11	0.29	725	706	253.8	—
91	12	2.19	0.17	0.39	635	553	360.1	—
92	12	2.01	0.17	0.35	704	717	315.8	—
93	12	2.0	0.074	0.31	701	623	330.3	—
94	12	1.8	0.012	0.27	709	589	180.9	—
95	12	2.0	0.11	0.29	717	603	298.7	—
96	12	2.0	0.048	0.3	741	610	256.0	—
97	12	2.0	0.048	0.19	701	582	256.0	—
98	12	2.0	0.0003	0.19	781	716	269.9	—

2). From this data, we will obtain a proper frictional loss coefficient to evaluate the pressure drops between points 2 and 5 and 6 and 3.

For a bare section between Z_1 and Z_2 the accelerational and gravitational components of the pressure drop were calculated, assuming a homogeneous flow, and by integrating the corresponding pressure gradients (Hetsroni 1982) as follows:

$$\Delta P_a = \int_{Z_1}^{Z_2} \left(\frac{dP}{dZ}\right)_a dZ = \int_{Z_1}^{Z_2} d\left(\frac{G^2}{\rho}\right) = \frac{G^2}{\rho_{Z_2}} - \frac{G^2}{\rho_{Z_1}} \quad [1]$$

and

$$\Delta P_g = \int_{Z_1}^{Z_2} \left(\frac{dP}{dZ}\right)_g dZ = \int_{Z_1}^{Z_2} \rho g \, dZ = \rho_{AV} g (Z_2 - Z_1), \quad [2]$$

where G is the mass flux, ρ is the density, ΔP_a is the accelerational pressure drop, ΔP_g is the gravitational pressure drop, Z is the axial levation, 1 and 2 are the location of ports 1 and 2, and ρ_{AV} is the average flow density between Z_1 and Z_2. The homogeneous flow model is chosen for the calculation of ΔP_a and ΔP_g since it gives better results for low pressures (Beattie 1973; Andeen & Griffith 1968). The experimental frictional pressure drop was then evaluated as

$$\Delta P_{f,exp} = \Delta P_{exp} - \Delta P_a - \Delta P_g, \quad [3]$$

where ΔP_{exp} is the measured total pressure drop and $\Delta P_{f,exp}$ is the experimental frictional pressure drop. The fluid properties required for such calculations depend mainly on the non-equilibrium vapor temperature which was measured at ports 2 and 3 only. At other locations (port 1, spacer inlet (5), spacer outlet (6)), however, the vapor temperatures were calculated using the model of Unal *et al.* (1991b), by evaluating the vapor generation rate in the dispersed flow regime, using the following energy balance equation:

$$G_v C_p \left(\frac{dT_v}{dZ}\right) + \Gamma [h_v(T_v, P_{sat}) - h_L] = 4\frac{Q}{D}. \quad [4]$$

In [4], Γ is the volumetric rate of vapor generation (Unal *et al.* 1991b), G_v is the vapor mass flow rate, T_v is the vapor temperature, h_v is the enthaply of vapor at (T_v, P_{sat}), h_L is the enthaply of liquid at (T_{sar}, P_{sat}), C_p is the vapor specific heat at constant pressure, D is the mean hydraulic diameter and Q is the heat flux.

Equation [4] is an initial value problem, and was solved iteratively by numerical integration over each of the sections (port 1–port 2), (port 2–spacer inlet (5)) and (spacer outlet (6)–port 3) of the bare rod bundle. Thus, the vapor temperatures at points 1, 5, and 6 were calculated from the measured values at points 2 and 3.

Figure 3 shows the friction factor (F_{exp}) corresponding to the present experimental data for the bare bundle calculated from its basic definition (Hetsroni 1982):

$$\left[\frac{dP}{dZ}\right]_{f,exp} = \frac{\Delta P_{f,exp}}{(Z_2 - Z_1)} = \frac{2F_{exp}G^2}{\rho_{AV}D}. \quad [5]$$

Since the flow regime is a dispersed flow and the distance between the pressure ports is small, the use of average density in [5] will not yield significant uncertainty. The experimental data is shown

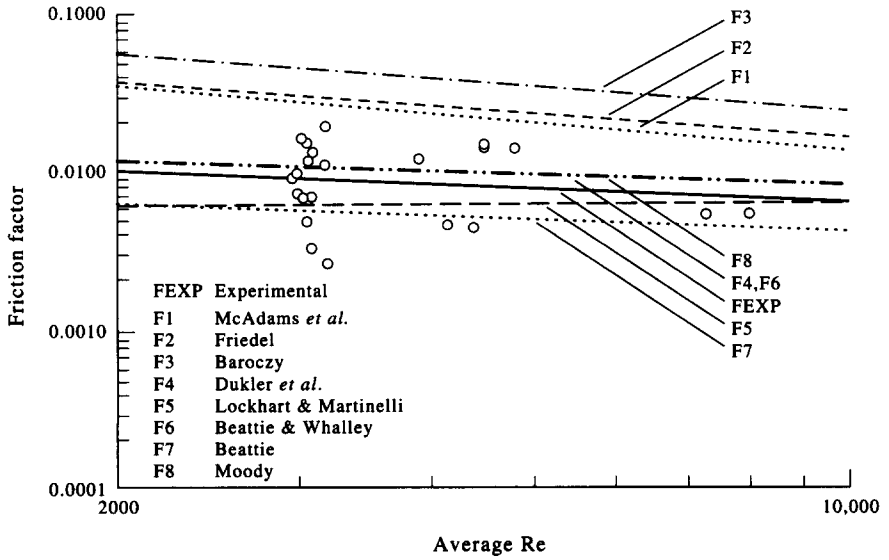

Figure 3. Friction factor of the bare rod bundle.

with circles and the best fit is represented by the solid line. For the purpose of comparison, the figure also shows the Moody friction factor for smooth pipes as well as the friction factor predicted by some of the well-known two-phase models for the present test conditions. It is very clear from the figure that the models of McAdams (1942), Friedel (1979) and Baroczy (1965) overestimate substantially the experimental friction factor and may not be applicable for the present test conditions. On the other hand, the friction factors predicted by the models of Dukler *et al.* (1964), Lockhart & Martinelli (1949), Beattie & Whalley (1982), Beattie (1973) (dry wall) and Moody (1944) (smooth pipe) compare reasonably with the present data. However, for better accuracy of the subsequent calculations in the grid spacer, it was decided to use the following correlation which fits the present data best:

$$F_{\text{exp}} = 0.10\ \text{Re}_{\text{AV}}^{-0.3}, \qquad [6]$$

where $\text{Re}_{\text{AV}} = GD/\mu_{\text{AV}}$; the viscosity ($\mu_{\text{AV}}$) is the arithmetic average of its values at the inlet and outlet of the section under consideration.

The observed scatter in the data is characteristic of two-phase flows in complex geometries, such as the one considered here (Beattie 1973; Hetsroni 1982). This scatter may be attributed to (a) the flow oscillations which were observed through a sight glass, (b) possible transient non-uniformities over the bundle cross section, (c) non-uniform impingement of liquid droplets or globules of the dispersed flow on the test rods and the shroud, (d) possible blockage of the transducer lines located at port 1 by liquid droplets etc. The minimum standard deviations of the experimental data from the predictions of [6] were calculated as 0.0011. When [6] for the friction factor was used in subsequent calculations of the spacer pressure drop, the effect of this standard deviation (0.0011) on the spacer pressure drop was found to be 7%.

The spacer loss coefficient data are presented in figure 4 as a function of the Reynolds number upstream of the spacer inlet (Re_5). The figure also shows the corresponding values predicted by the models of Rehme (1977). Yao *et al.* (1982) and Beattie (1973). The fluid properties used in the spacer calculations were those at the upstream end of the grid spacer (elevation 5). Despite having the same trends, the three models substantially underpredicted the present spacer loss coefficients. Rehme's (1977) model and Yao *et al.*'s (1982) model, which is suggested to be 50% higher than Rehme's (1977), were developed on the basis of experimental data of incompressible single-phase flows. On the other hand, Beattie's (1973) model was derived from the mixing-length theory for a churn-turbulent flow at an obstruction. The disagreement between Beattie's prediction and the present data can be attributed to differences in the thermal hydraulic conditions in the churn and dispersed flow conditions in the spacer. Unfortunately, the flow patterns, thermal conditions and parametric ranges of applicability of such a model (particularly whether or not the flow was

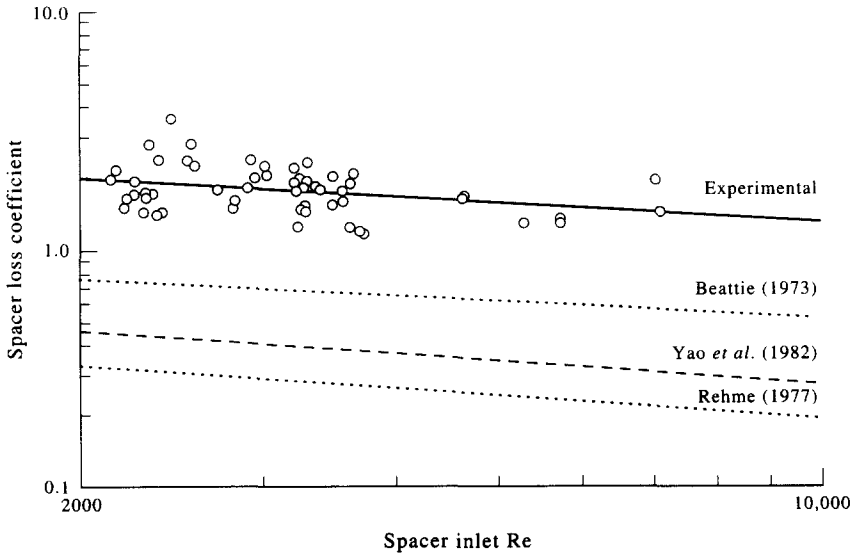

Figure 4. Pressure loss coefficient of the grid spacer.

adiabatic) were not identified. We should note that one of the important points to remember is that the heated shroud eliminates the possibility of cross flow in the present tests.

SUMMARY AND CONCLUSIONS

In the present experimental program of post-CHF dispersed flow in a 3 × 3 rod bundle with a grid spacer, measurements of heat flux, mass flux, wall temperatures, non-equilibrium vapor temperatures and total pressure drop were taken across two sections of the rod bundle. The first section without a spacer (1–2) was used to evaluate the most appropriate model for the friction factor in the bare rod bundle, while the second one (2–3) with a blocked bundle was used to evaluate the pressure drop in the grid spacer under different test conditions.

Comparison of the present data with well-known models of the friction factor in a bare rod bundle showed poor agreement with three models and reasonable agreement with four other models. However, the model which best fitted the present data for the friction factor was used for subsequent calculations in the blocked section.

The pressure drop in the grid spacer was calculated from the experimental data by subtracting the gravitational, accelerational and frictional components in the unblocked parts of the section (2–3). When compared to the present data the available models showed the right trend, but substantially underpredicted the present spacer loss coefficient and two-phase multiplier. It is suggested that pressure drop values, which are 300% higher than those predicted by Beattie's (1973) model, may be used for post-CHF dispersed flow in grid spacers. The large deviations between the experimental data and the models were attributed mainly to the differences in the flow pattern and thermal conditions in the spacer.

Acknowledgements—This work was partially supported by the U.S. Nuclear Regulatory Commission under Contract No. NRC-04-81-183. The authors acknowledge the help by L. E. Hocreither of Westinghouse Electric Corporation in providing the grid spacer.

REFERENCES

ANDEEN, G. B. & GRIFFITH, P. 1968 Momentum flux in two-phase flow. *J. Heat Transfer* **90,** 211–222.

BADR, O., UNAL, C., TUZLA, K., NETI, S. & CHEN, J. C. 1993 Pressure drop in rod bundle spacers in post-CHF dispersed flow regime. In *Proc. 29th Am. Nucl. Soc. Natn. Heat Transfer Conf.*, pp. 108–115.

BAROCZY, C. 1965 A systematic correlation for two-phase pressure drop. *Chem. Engng Prog. Symp. Ser.* **62,** 232–249.

BEATTIE, D. 1973 A note on the calculation of two-phase pressure losses. *Nucl. Engng Des.* **25,** 395–402.

BEATTIE, D. & WHALLEY, P. 1982 A simple two-phase frictional pressure drop calculation method. *Int. J. Multiphase Flow* **8,** 83–87.

DE STORDEUR, 1961 Drag coefficients for fuel-elements spacers. *Nucleonics* **19,** 74.

DUKLER, A., WICKS, M. & CLEVELAND, R. 1964 Pressure drop and holdup in two-phase flow. *AIChE Jl* **10,** 38–51.

FRIEDEL, L. 1979 Improved friction pressure drop correlation for horizontal and vertical two-phase flow. Presented at the *Eur. Two-phase Flow Gp Mtg*, Ispra, Italy, paper E2.

HETSRONI, G. 1982 *Handbook of Multiphase Systems*, pp. 2.44–2.75. McGraw–Hill, New York.

LOCKHART, R. & MARTINELLI, R. 1949 Proposed correlation of data for isothermal two-phase two component flow in pipes. *Chem. Engng Prog.* **45,** 39–48.

MCADAMS, W., WOODS, W. & HEROMAN, L. 1942 Vaporization inside horizontal tubes, 2: benzene–oil mixtures. *Trans. ASME* **64,** 193–200.

MOODY, L. 1944 Friction factors for pipe flow. *Trans. ASME* **66.**

REHME, K. 1973 Pressure drop calculations for fuel elements spacers. *Nucl. Technol.* **17,** 15–23.

REHME, K. 1977 Pressure drop of spacer grids in smooth and roughened rod bundles. *Nucl. Technol.* **33,** 314–317.

SANGSTER, W. 1968 Calculation of rod bundle pressure losses. Report ASME-68-WA/TH-35.

UNAL, C., TUZLA, K., BADR, O., NETI, S. & CHEN, J. C. 1986 Experimental study of non-equilibrium post-CHF heat transfer in rod bundles. In *Proc. 8th Int. Heat Transfer Conf.*, Vol. IV, pp. 2417–2422.

UNAL, C., TUZLA, K., BADR, O., NETI, S. & CHEN, J. C. 1988a Parametric trends for post-CHF heat transfer in rod bundles. *J. Heat Transfer* **110,** 721–727.

UNAL, C., TUZLA, K., BADR, O., NETI, S. & CHEN, J. C. 1988b Convective film boiling in a rod bundle: axial variation of non-equilibrium evaporation rates. *Int. J. Heat Mass Transfer* **31,** 2091–2100.

UNAL, C., TUZLA, K., BADR, O., NETI, S. & CHEN, J. C. 1991a Convective film boiling in a rod bundle: transverse variation of vapor superheat temperature under stabilized post-CHF conditions. *Int. J. Heat Mass Transfer* **34,** 1695–1706.

UNAL, C., TUZLA, K., COKMEZ-TUZLA, A. F. & CHEN, J. C. 1991b Vapor generation rate model for dispersed drop flow. *Nucl. Engng Des.* **125,** 161–173.

YAO, S., HOCHREITER, L. E. & LEECH, W. 1982 Heat transfer augmentation in rod bundles near grid spacers. *J. Heat Transfer* **104,** 76–81.